

## NUMERICAL MODELLING OF THE PROCESS OF COLD PLASTIC DEFORMATION WITH PLANETARY ROLLERS

Gina Mihaela Sicoe, Iacomi Doina, Iordache Monica, Nitu Eduard

<sup>1</sup>University of Pitesti-Romania, Department of Manufacturing and Industrial Management  
Pitesti, Riurilor Street, No.20, 110036 Pitesti, Romania

Corresponding author: Gina Mihaela Sicoe, gina\_boicea@yahoo.com

**Abstract:** Numerical simulation allows a significant improvement of the stage of conceiving technologies based on these processes by analysing a great number of variants, for a wide range of variation of process parameters to find the optimal solution. The time and cost to validate the solution chosen, as compared to experimental research are diminished when using the numerical simulation. As well, simulation allows establishing the limits to apply the process according to profiles, materials, equipment and tools. In this context, it is considered that the research connected to the numerical modelling of the deformation process with planetary rollers is timely and useful for industry. Models obtained after the numerical simulation are useful for technology designers in order to avoid risks and find the optimal solution for a given case.

The purpose of this paper was to validate more numerical models and to establish the correct value of the friction coefficient between the rollers and the semi product for the process of cold deformation with planetary rollers. In order to reach this objective simulations were performed on pieces obtained from two types of steel AISI1015 and AISI1040 for two types of profiles commonly used in industry: metric and trapezoidal.

**Key words:** plastic behaviour of the material, cold plastic deformation with planetary rollers, numerical modelling, friction coefficient, Abaqus.

### 1. INTRODUCTION

The objective of the research conducted in this paper consisted in developing a numerical model to allow performing simulations in order to find a solution without risks and establishing the best choice in a given case, when processing profiles by cold rolling with planetary rollers. Reaching this objective will allow those who conceive technologies to process by cold deformation to simulate this process in order to obtain pieces which will meet the requirements imposed in connection with the quality of the pieces. Industrial processes meant to achieve profiled parts are in a continuous development and competition for high quality and cost of products. Effective processes must be used in order to reach these goals.

The form tapping process with planetary rollers is

one of the processes used to obtain different types of profiles in solid or hollow cylindrical pieces of larger sizes and diameters by comparison to other cold deformation processes.

The tendency is to develop and implement numerical modelling which is a very useful and efficient tool successfully replacing experimental research and development. The experimental study of the deformation process (equipment kinematics, tool geometry, technological parameters etc.) represents a laborious activity requiring time, materials and energy. This is why the process can be studied efficiently by numerical simulation and modelling.

The simulation of some complex processes with numerical modelling has become possible due to important progress made in the field of material deformation mechanics, increase of storage capacity and processing information by modern computing tools (Warrington, 2006). As well, many programmes, more or less specialised, based on the finite element were developed to model the processes (Warrington, 2006).

Although the finite element modelling of the form tapping process began in the 1990, the studies were limited by the high volume of calculations and the computers incapacity to simulate the process within a reasonable time.

In 2000, the development of efficient FE software and the increasing computational capacity of computers produced an intensification of researches (Warrington, 2006). The researches focused on the material of the work-piece, the piece profile and the rolling process, especially the plastic behaviour of the material, the meshing elements and the software used for simulations (MARC, ABAQUS, DEFORM, MSC Super Form).

The strain-hardening laws of Hollomon, Ludwik, Ludwik-Hartley and Voce were most frequently used to analyse and simulate large plastic deformations at room temperature. However, cold rolling processes are influenced by the effects of high-speed processing and accompanied by an increase of temperature;

because there is not enough time for the heat generated by plastic deformation to be evacuated by convection through the surface and by conduction to the connecting parts. Johnson-Cook's law (Johnson) is often used to describe the effects of strain-rate and temperature.

This paper studies the development of three-dimensional FE models using the stress-strain law described by compression tests and an optimal mesh of the work-piece for accurate results to be obtained with a reasonable number of elements and an acceptable computation time.

## 2. EXPERIMENTAL PROCEDURE

The diagram to generate a profile corresponds to the one presented in figure 1. The rolling head with radius  $R$ , rotates with the speed of revolutions  $n$ , the rollers with radius  $r$  are free on their axis so that at contact with the material of the piece they can rotate.

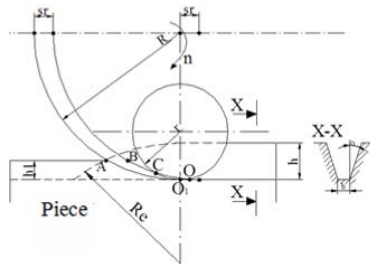


Fig.1. The forming process in an early stage

With each rotation the head advances on the direction of the profile to be achieved with the feed  $s_r$ , and a roller with radius  $r$  moves the material from section  $OO_1ABO$  towards the exterior, so that in the area of maximum penetration of the roller into the material (vertically) the profile is obtained on arc  $OO_1A$ . The contact of the roller with the piece, for the forming position in figure 1, takes place on arc  $O_1C$ . The profile with depth  $h$  can be followed in section  $X-X$ . The penetration of the roller into the semi product takes place at depth  $h_1$ , and at some point in the forming process, the surface of the profile crests nearly follows radius  $R_c$ . When rotating the rolling head the forming process continues by forming roller  $r$  on arc  $O_1A$ , so that point  $C$  reaches  $B$ . Theoretically, from this point the process follows line  $BA$ .

When forming the roller with radius  $r$ , on arc  $OO_1A$ , the parameters which define the volume of deformed material are variable:

- thickness  $g$  of the section of deformed material, figure 2, which increases from zero to a maximum value and then decreases again to zero;
- area  $S$  of the deformed material, which increases from zero in section  $X-X$  to a maximum value in the section where  $g$  has a maximum value;

- length of the contact arc  $O_1C$  between the roller and the piece,  $l_c$ , which varies from zero to value  $O_1C$ , remains constant at this value until point  $C$  reaches  $B$ , then decreases again to zero.

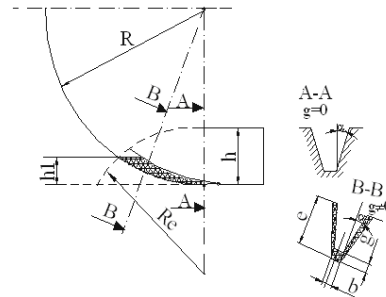


Fig. 2. Area of the material deformed in two sections

The analysis of the evolution in time of the three parameters which influence the forming force, detailed in (Iordache 2011) showed that there is a relation of dependence in the form of that presented in figure 3.

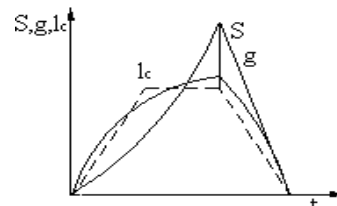


Fig. 3. The evolution in time of parameters  $g$ ,  $S$ ,  $l_c$

Since the forming force is determined by the volume of material deformed by the roller at a certain point, the parameters which determine the volume of material will also determine the forming force. By analysing the evolution of the three parameters, it results that the forming force will be variable, it starts from zero, at the first contact of the roller with the piece, it increases to a maximum value corresponding to the situation when the roller reaches  $g$ , and then, the force decreases reaching zero, at the loss of contact between the roller and the piece. We can conclude that for a geometry given by the rolling head, the forming force depends on:

- feed  $s_r$  [mm/rot];
- depth of penetration  $h_1$  to achieve the profile;
- geometry of the forming profile, expressed by parameters  $b$  and  $\alpha$  respectively;
- a parameter which characterizes the material, usually its hardness.

### 2.2 Materials, pieces and profiles processed

The materials for the pieces formed chosen were two types of steel: AISI1015 and AISI1040. The materials used for the processing were chosen in order to have different mechanical properties in a wide range and to be representative for their group, table 1.

Table 1. Mechanical characteristics of the steel used

| Steel     | HB<br>[kg/mm <sup>2</sup> ] | HV <sub>0,3</sub><br>[kg/mm <sup>2</sup> ] | Rp <sub>0,2</sub><br>[N/mm <sup>2</sup> ] | Rm<br>[N/mm <sup>2</sup> ] | A5<br>[%] |
|-----------|-----------------------------|--|---|----------------------------|-----------|
| AISI 1015 | 156,1                       | 139  | 298                                       | 475                        | 15        |
| AISI 5140 | 277,4                       | 245,5                                      | 396                                       | 837                        | 7         |

The processed parts have a rectangular shape, figure 4, on each piece there are two areas where profiles can be processed. A working area has 25 mm and allows the processing of channels with constant parameters by removing the areas of entrance and exit of the head.

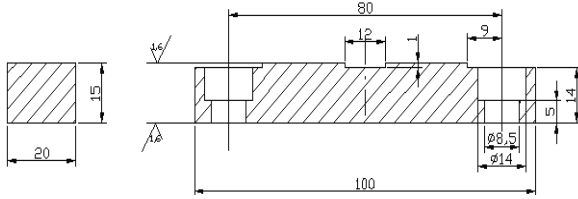


Fig. 4. Semi products used for the processing

Concerning the geometry of profiles, two profiles corresponding to threads M20, figure 5.a, and Tr20, figure 5.b, obtained at different depths were chosen. The processed profile is formed by 5 identical grooves in axial section to the one of the ISO metric thread M20x2 and Tr20, their geometry being presented in figure 5.

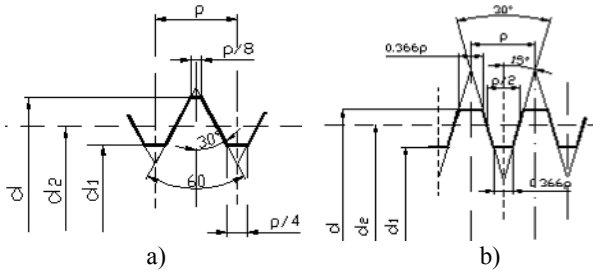


Fig. 5. Geometry of studied profiles

### 2.3 Experiment plans used

The experience plan was meant to vary two parameters for each one of the four materials: feed; depth of the processed profile. Each parameter varied on three levels, table 2.

Table 2 The experience plan used

| No. exp. | Speed of revolutions, n, [rot/min] | Feed, s <sub>i</sub> [mm/rot] | Processing depth, h <sub>1</sub> [mm] |
|----------|------------------------------------|-------------------------------|---------------------------------------|
| 1        | 235                                | 0,1                           | 0,3                                   |
| 2        |                                    | 0,2                           |                                       |
| 3        |                                    | 0,4                           |                                       |
| 4        |                                    | 0,1                           | 0,45                                  |
| 5        |                                    | 0,2                           |                                       |
| 6        |                                    | 0,4                           |                                       |
| 7        |                                    | 0,1                           | 0,675                                 |
| 8        |                                    | 0,2                           |                                       |
| 9        |                                    | 0,4                           |                                       |

## 3. NUMERICAL MODELLING

### 3.1 Numerical models developed

The researches on the numerical model to simulate the process of plastic intermittent deformation with planetary rollers to achieve profiles aimed on the one hand the accuracy of the results obtained through simulation and on the other hand to obtain simulation periods acceptable in practice. Following these aspects several models were taken into consideration during the researches.

A model, which encountered difficulties in assembling and imposing limit conditions, with which no significant results were obtained and which had a high calculating time did not perform any simulation.

The first model, called model 1, with which acceptable results were obtained is one in which a rolling head with 3 rollers was used, a cylindrical semi product and the kinematics of the process was replaced so that it reproduced the real process and maintained permanent contact between the rollers and the piece. With this model results close to the experimental ones were obtained, but the calculating time was high, 300 h.

A second model, model 2, developed and used in simulations to accurately describe the rolling process through intermittent blow performed experimentally. The tools were modelled as shell rigid elements; the semi product had small dimensions, a cuboids shape. The calculating time with this model was of about 90 h and due to the fact that the process took place quickly the frequency of acquiring rolling forces was not enough.

### 3.2 Process kinematics of model 1

For the modelling, the process was adapted so that the rollers do not lose contact with the semi product. In order to do so it started from the real process. This is carried out sequentially and over very small periods of time. At a rotation speed of 235 rotations per minute, the entire process takes about 0,01 seconds. The scheme of the rolling process, when a roller crosses, can be followed in figure 6.

For the roller to remain in continuous contact to the piece, in the numerical model it was considered that the piece is cylindrical, has bores and its diameter is equal to that of the rolling head. To simulate the rolling process, it was considered that the roller moves towards the exterior following the law imposed by thickness g on its ascending curve during the rotation of a piece. During the next rotation the roller does not advance any more. During this time it reaches again the cylindrical shape. If the head will have three rollers placed equidistant angular and axial with the pass between profiles to form three channels the sequential process of achieving three channels

inside the piece is simulated.

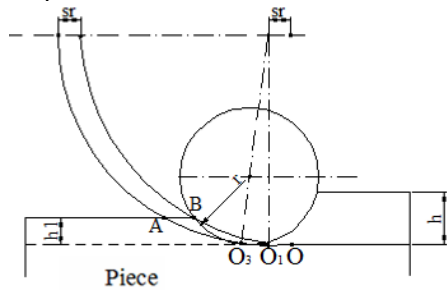


Fig. 6. Rolling process with the roller in the maximum section of material

When rolling the roller with radius  $r$  on arch  $OO_1A$ , the parameters which define the volume of deformed material vary:

- thickness  $g$  of section  $OO_1ABO$  increases from zero to a maximum value and then goes back to zero, figure 7;
- section  $S$  of the material deformed at a certain point varies during the entire rolling;
- length of contact arch  $O_1C$ , of the roller with the piece varies from zero to value  $O_1C$ , remains constant at this value until point  $C$  reaches  $B$ , then it decreases to zero again.

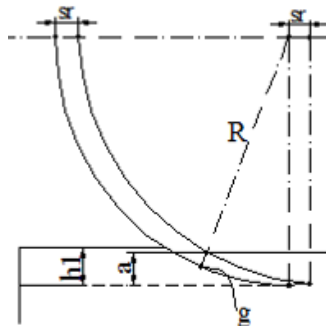


Fig. 7. Thickness of the material deformed at one rolling in the bottom area of the profile

The value of  $g$  is given by relation:

$$g = R - \sqrt{R^2 - 2 \cdot s_r \cdot \sqrt{2 \cdot R \cdot a - a^2} + s_r^2} \quad (1)$$

As it can be noticed from the relation, the maximum thickness of deformed material for a dimension  $R$  of the rolling head depends on the feed on a rotation of the head and the penetration depth of the roller in the material to achieve the profile. At the increase of the two parameters,  $g$  increases reaching the maximum value for the situation in which  $a$  becomes equal to  $h_1$ . It is obvious that for this situation the rolling force will also be maximal.

According to the previous description, the law of radial penetration of the rollers has the form presented in figure 9.

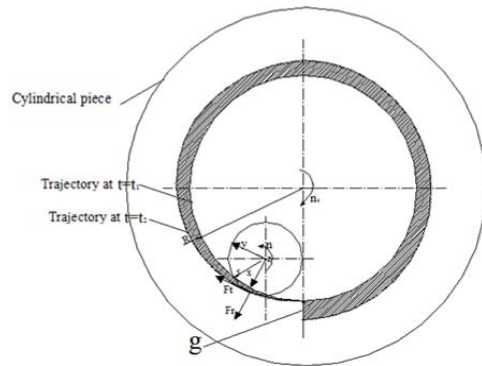


Fig. 8. Penetration of the roller in the first rotation in the replacement process

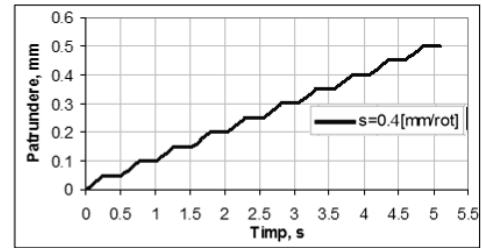


Fig. 9. Law of penetration of the rollers in the piece for the replacement process,  $s_r = 0,4$

### 3.3 Process kinematics of model 2

The kinematics used in model 2 describes the experimental conditions. The semi product is deformable and has a cuboids shape. It has small dimensions (10 mm x 5 mm x 6 mm), in order to be meshed into small finite elements, but few overall, to reduce the calculating time. The three tools have the same shape and dimensions as those used for the previous model, figure 10.

The rolling head has three rollers and rotates with the speed  $n_c$  and the piece moves tangential to the rolling head with feed  $s$ . The rollers rotate freely around their own axes.

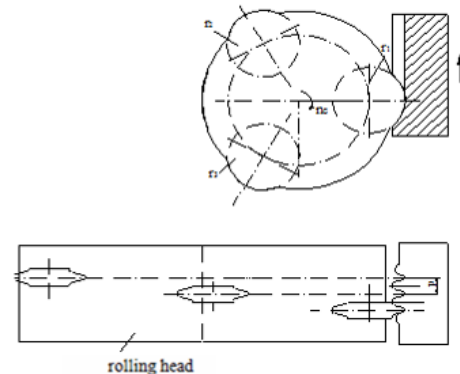


Fig. 10. Kinematics of model

## 4. CONSTRUCTING NUMERICAL MODELS

### 4.1 Principles used to construct models

For the numerical modelling of the rolling process through intermittent blow, the conclusions drawn at

the simulation of the radial rolling process with roller tools represented the starting point [FLO 11]:

- the optimal meshing of the semi product consists in dividing the semi product in six different areas associated to some areas with different levels of deformation;
- the law of behaviour of the piece material is the one which combines Hollomon and Voce's laws, established based on compression tests performed at low deformation speeds;
- the use of an explicit analysis to solve the equations of the model.

#### 4.2 Constructing numerical model 1

The semi product used for the simulation has a cylindrical shape; the profile is achieved on the inside and is defined as being a "deformable body", figure 11.

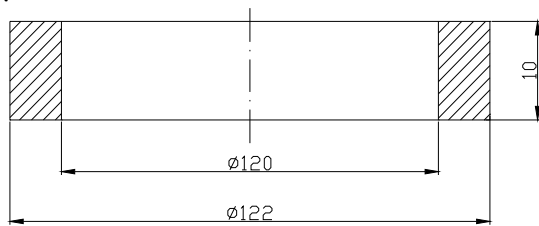


Fig. 11. Shape of the semi product used for model 1

The thickness of the semi product is of 10 mm to allow obtaining three profiles. There was chosen a number of three profiles, instead of five (used experimentally) to reduce the calculating time.

"Shell" type of tools is modelled with the help of rigid elements and has the profile combined with the one to achieve and the exterior diameter has 40 mm, figure 12.

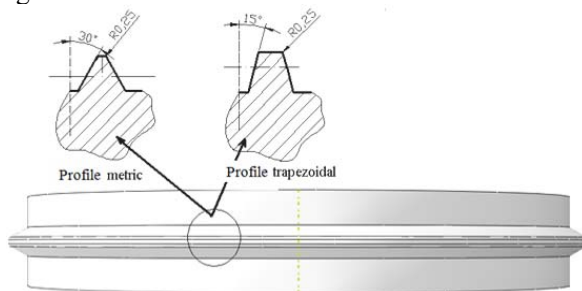


Fig. 12. Profile of the tools used

The mesh has to be made so that the calculating time is reasonable, but the number of elements is enough to render as close as possible the real state of tensions and deformations in the deformed piece in a reasonable time.

At the mesh of the semi product, the conclusions drawn at the simulation of the radial rolling were taken into consideration. Therefore, the semi product was divided into specific areas according to the deformation degree and profile dimensions. On an axial direction three areas were made, figure 13:

- area A, with very small deformations, where the dimension of the elements can be very big;
- area B, corresponding to the profile gap, highly deformed, where the size of the elements has to be as small as possible, was divided in two differently meshed areas: area B<sub>1</sub>, corresponding to the profile gap, with the highest deformations, which is very smoothly meshed and area B<sub>2</sub>, corresponding to the profile flank, with high deformations, which is smoothly meshed;
- area C, corresponding to profile top, with low deformations, where the size of the elements is average.

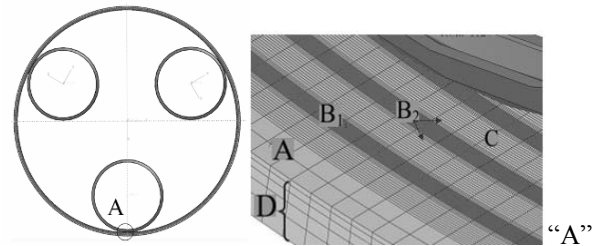


Fig. 13. Mesh manner for model 1

On a radial direction, area D was achieved associated to the superficially deformed layer, where the size of the element has to be small. In this area a progressive mesh with 5 elements was performed where the ratio between sides is 3.

#### 4.3 Constructing numerical model 2

Model 2 describes experimental conditions. The semi product is deformable and has a cuboids shape of small dimensions (10 mm x 5 mm x 6 mm) to reduce the calculating time. The three tools have the same shape and dimensions as those used for model 1. The mesh of the semi product was performed by dividing areas specific to the degree of deformation, figure 14.

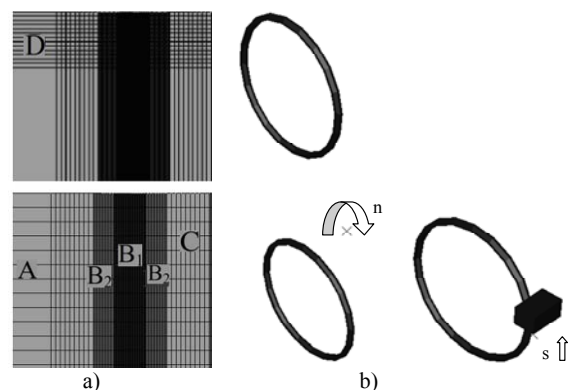


Fig. 14. Numerical model 2 a) semi product mesh; b) model kinematics

For all areas A, B, C and D hexahedral solid elements with 8 nodes and reduced integration – C3D8R are used.

The parameters of the rolling head are introduced in the model by establishing limit conditions, figure 14. b:

- the tools rotate around the central axes system,  $n=475$  rot/min;
- the semi product moves with the same feed as the experimental one ( $s = 0,1$  mm/rot,  $s = 0,2$  mm/rot,  $s = 0,4$  mm/rot etc.).

The contact between surfaces is of the type “surface-to-surface”, the friction coefficient between the tools and the semi product is 0. (Boicea, 2011)

#### 4.4 Behaviour laws of materials used for plastic deformation

The behaviour laws of materials at plastic deformation set and used in paper (Marincei 2010) for radial rolling with disk rollers were used.

Materials behaviour, in this paper, was set as follows:

- using Young’s modulus Young  $E = 210$ GPa and Poisson’s coefficient  $\nu = 0,3$ , in the elastic domain;
- using the behaviour law combining Hollomon and Voce’s laws, in the plastic domain.

The results obtained at the simulation of the radial rolling process (Marincei 2010) validated this law. The compression test at low speeds for steels AISI1015 and AISI10 was used in order to determine experimentally the coefficients of these laws:

$$\sigma_{AISI1015} = [542,5 \cdot \varepsilon^{0,135} + 217,6(1 - 0,99 \exp(-9,91 \cdot \varepsilon))] \quad (1)$$

$$\sigma_{AISI1040} = [673,8 \cdot \varepsilon^{0,022} + 371,8(1 - 0,99 \exp(-15,61 \cdot \varepsilon))] \quad (2)$$

### 5.SIMULATIONS TO VALIDATE THE MODEL

#### 5.1 Objective of simulations and simulation plan

The simulations aimed to validate the numerical models achieved. The validation of the numerical models achieved requires a comparison between the entire assembly of results obtained through numerical simulation and those obtained experimentally.

The following aspects were taken into consideration for the comparison:

- the evolution and values of the rolling forces;
- the level of equivalent deformations at the end of the process, of other parameters which can be deduced from these deformations;
- the behaviour laws of the materials deformed.

The plan used in the experimental research of the process was considered when the simulation plan was established in order to obtain the data required for the validation of the models achieved.

The plan used for the simulations is presented in table 3. The two established models and different values of the friction coefficients were used for the simulations.

Table 3. The simulation plan

| No. of sample | Material piece | Type of profile | The experimental parameters |                |        |
|---------------|----------------|-----------------|-----------------------------|----------------|--------|
|               |                |                 | n [rot/min]                 | $s_r$ [mm/rot] | h [mm] |
| 1             | OLC15          | M20             | 235                         | 0,4            | 0,485  |
| 2             | OLC15          | M20             | 235                         | 0,1            | 0,481  |
| 3             | OLC15          | Tr20            | 235                         | 0,1            | 0,501  |
| 4             | OLC15          | Tr20            | 235                         | 0,1            | 0,698  |
| 5             | 40Cr10         | M20             | 235                         | 0,4            | 0,4833 |
| 6             | 40Cr10         | Tr20            | 235                         | 0,4            | 0,495  |
| 7             | 40Cr10         | Tr20            | 235                         | 0,4            | 0,7    |

#### 5.2 Results obtained at simulations with numerical model 1

The 6 samples were simulated with numerical model 1, for which there is the entire assembly of data required to validate the models.

Another sample, sample 1, was simulated with model 1 for two values of the friction coefficient:  $\mu = 0$  and  $\mu = 0,3$ , respectively.

The values of the maximum radial forces obtained are presented in table 4. The errors obtained are smaller when using a friction coefficient equal to 0.

Table 4. Values of maximum forces

| No. of sample | Material piece | $\mu$ | h, [mm] | $F_{max}$ [KN] |      | Error [%] |
|---------------|----------------|-------|---------|----------------|------|-----------|
|               |                |       |         | exp.           | sim. |           |
| 1             | OLC15          | 0,3   | 0,3     | 3,53           | 3,10 | 12,2      |
|               |                |       | 0,5     | 4,83           | 4,87 | 0,83      |
|               |                | 0     | 0,3     | 3,53           | 3,36 | 4,82      |
|               |                |       | 0,5     | 4,83           | 4,43 | 8,28      |

The evolution in time of the two components of the rolling force obtained after the simulation for the metric profile, friction coefficient  $\mu = 0$  can be followed in figure 15, and for the friction coefficient  $\mu = 0,3$  in figure 16.

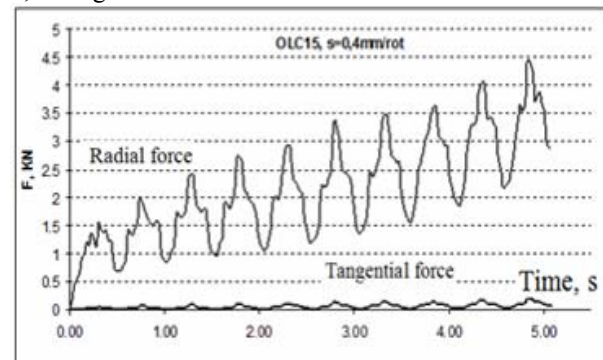


Fig. 16. Evolution of the forces obtained at simulation with model 1,  $\mu = 0$

For the friction coefficient  $\mu = 0,3$ , the tangential component has a value of over 30% of the radial one, unnatural thing if we take into account the experimental measurements.

The experimental measurements showed that the tangential force is practically negligible. This means that the use of the friction coefficient  $\mu = 0$  is correct.

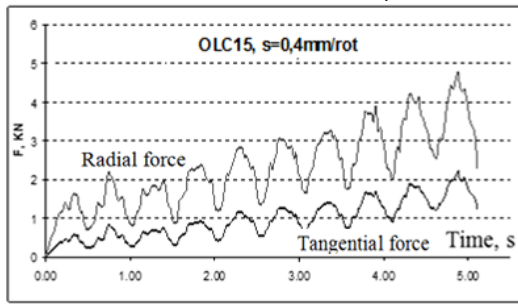


Fig. 17. Evolution of the forces obtained at simulation with model 1,  $\mu = 0,3$

The parameter based on the analysis of the degree and manner of strain hardening of the deformed layer was also used for the validation of the numerical model. On the one hand, the experimental values of the micro hardness of the strain hardened layer measured in the axial section of the profile and on the other hand, the values of the equivalent deformations  $\bar{\epsilon}$  (PEEQ) in the same area of the profile, obtained through simulation, were used for this objective. Based on some hypotheses (TAB 1951), the two values (HV and  $\bar{\epsilon}$ ) were transformed into values directly comparable, into tensions, respectively, expressed by the same measuring unit [MPa].

The deformations obtained through simulation with model 1 for friction coefficients  $\mu = 0$  and  $0,3$ , respectively, profile depth  $0,5$  mm, OLC15-M20- $s=0,4$ mm/rot, are presented in figure 18.

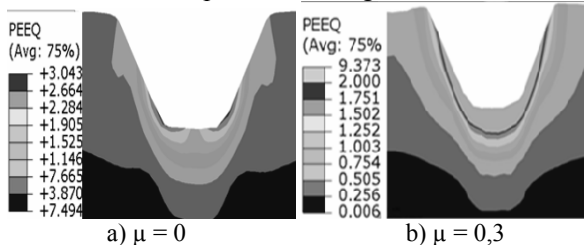


Fig. 18. Deformations obtained through simulation with model 1

Analysing the deformations obtained through simulation for the two friction coefficients (figure 18) it results that for the friction coefficient  $\mu = 0,3$ , in the superficial layer of the profile, the material suffered high deformations, over the breakage limit. This fact is not confirmed by the experiments performed. It is due to the tangential force determined by the high friction coefficient taken into consideration at simulation.

### 5.3 Results obtained at simulations with numerical model 2

The 6 samples, 2, 3, 4, 5, 6, 7, were simulated with the numerical model 2 for the friction coefficient  $\mu =$

$0$ , coefficient which turned to be correct.

The values of the maximum forces obtained experimentally, through simulation with model 2, for samples 2, 3, 4, 5, 6 and 7 are presented in table 5.

Table 5 Values of maximum forces

| No. of sample | Material piece | Type of profile | h, [mm] | F <sub>max</sub> exp. [KN] | F <sub>max</sub> sim. [KN] | Error, [%] |
|---------------|----------------|-----------------|---------|----------------------------|----------------------------|------------|
| 2             | OLC15          | M20             | 0,5     | 3,36                       | 3,95                       | 17,56      |
| 3             |                | Tr20            | 0,5     | 2,98                       | 2,85                       | 4,36       |
| 4             | 40Cr10         | Tr20            | 0,7     | 3,27                       | 3,4                        | 3,98       |
| 5             |                |                 | M20     | 0,5                        | 7,54                       | 7,4        |
| 6             | 40Cr10         | Tr20            | 0,5     | 6,52                       | 7,79                       | 19,47      |
| 7             |                |                 | 0,7     | 7,55                       | 9,2                        | 21,85      |

Both models can be validated by taking into account the fact that the errors between the maximum values of the forces obtained by simulation with the two models and experimentally vary between 1,86% and 21,85%.

The distributions of equivalent deformations obtained through simulation with model 2 and experimentally for sample 2 are presented in figure 19.

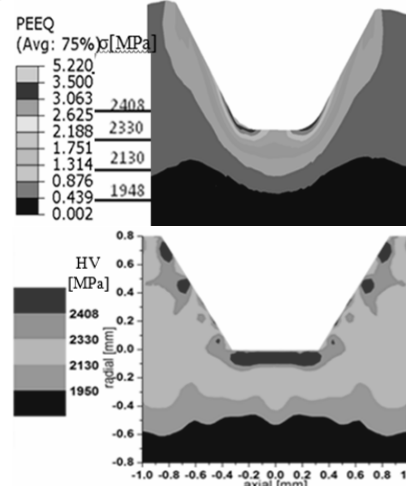


Fig. 19. Distributions of equivalent deformations obtained through simulation with model 2 and experimentally for sample 2

General shape of the deformation field obtained on the metric profile is comparable to the one obtained on the trapezoidal profile. Compared to profile M20 processed on the same material and under the same technological conditions it is pointed out by a higher strain hardening of the gap and base flank of the profile and by a lower strain hardening of the central area of the tooth, aspect found in experiments as well.

## 6. CONCLUSIONS

The researches performed to achieve the numerical model for the simulation of the process of intermittent plastic deformation with planetary rollers

to obtain profiles focused, on the one hand, on the accuracy of the results obtained through simulation and, on the other hand, on the acceptable simulation periods for practice. Two models were considered in the researches.

Model 1: a rolling head with 3 rollers, a cylindrical semi product were used, the kinematics of the process was replaced in order to reproduce the real process and permanent contact was maintained between the rollers and the piece; acceptable results were obtained, but the calculating time was high, about 300h.

Model 2: the tools were modelled as shell rigid elements; the semi product had small dimensions and a cuboids shape; the computing time with this model was of about 90h; the process took place quickly and the frequency to acquire the rolling forces was not enough.

In this paper, simulations focused on the validation of the numerical models achieved by comparing the results obtained by numerical simulation with those obtained experimentally. Two important process parameters were compared: evolution and values of rolling forces; degree of equivalent deformations at the end of the process, of other parameters which can be deduced from these deformations and the behaviour laws of the materials to be deformed.

A very good correspondence is achieved between the forces obtained experimentally and those obtained through simulation if the forces recorded experimentally for depths of 0,3 mm and 0,5 mm, respectively, are overlapped with the graph of force evolution when  $\mu = 0$ .

Next, the parameter based on the analysis of the degree and manner of strain hardening of the deformed layer was used to validate the numerical model. On the one hand, the experimental values of the micro hardness of the strain hardened layer measured in the profile flank and in the axial section of the profile and, on the other hand, the values of equivalent deformations (PEEQ) in the same area of the profile, obtained through simulation, were used.

From the analysis of the deformations obtained through simulation for the two friction coefficients, it results that for the friction coefficient  $\mu = 0,3$ , in the superficial layer of the profile, the material underwent high deformations, over the breakage limit. Due to the tangential force determined by the high friction coefficient considered at simulation, experiments do not confirm this aspect. Again, it results that zero is the correct friction coefficient which has to be used for simulation. The simulation plan was wide enough concerning samples of materials with extreme characteristics (AISI1015 and AISI1040) on the two profiles, metric and trapezoidal, different values of the working feed and of the penetration depth of the profile. By comparing

the results obtained through simulation related to the forces, deformations and tensions both with model 1 and 2, to those obtained experimentally, it can be noted that both models are accurate enough to simulate the process.

## 7. REFERENCES

1. Boicea, G., (2012). *Cercetări privind modelarea numerică a procesului de deformare la rece prin rulare cu role planetare pentru realizarea de profile*. Ph.D. Thesis, University of Pitești.
2. Boicea, G., Ungureanu, I., Iordache, M., Nițu, E., Iacomi, D., Tudor, M., (2012). *Experimental Research On The Quality Of Profiles Obtained By Form Tapping*, Proceedings of ModTech-New face of TMCR, Vol. I, ISSN: 2069-6736, pp.133-136.
3. Boicea, G., Ungureanu, I., Nițu, E., Iordache, M., (2011). *Numerical simulation using the fem of the cold plastic deformation process with planetary rollers to achieve profiles*. University of Pitesti Scientific Bulletin, Automotive Series A, No. 20.
4. Boicea, G., Ungureanu, I., Nițu, E., Iordache, M., (2011). *Finite element modelling of cold rolling by form tapping of grooves*. Academic Journal of Manufacturing Engineering, vol. 9, ISSUE 4/2011, ISSN 1583-7904, pp. 18-23.
5. Domblesky, J. P., Feng, F., (2002). *A parametric study of process parameters in external thread rolling*, Journal of Materials Processing Technology, pp. 341–349.
6. Iordache, M., Ungureanu, I., Boicea, G., Nitu, E., Iacomi, D. (2011). *Experimental study of the rolling forces on profiles form tapping*, Academic Journal of Manufacturing Engineering, Vol. 7, Issue 1, pp. 77-82.
7. Marinței, L., Iordache, M., Nițu, E., Ungureanu, I., Boicea, G., (2010). *Theoretical and experimental studies for the behavior determination of some steels at the cold plastic deformation*, Proceedings of ModTech-New face of TMCR, pp. 367-369.
8. Nițu, E., Ungureanu, I., Iacomi, D., Tabacu, Șt., Iordache, M., Marinței, L. (2011). *Modelarea analitică și numerică a proceselor de deformare plastică volumică la rece a profilelor*, Final Research Report, Project PN II IDEI 711\_2008, Pitești.
9. Tabor, D., (1951). *The hardness and strength of materials*, Journal of the Institute of metals, Vol. 79, pp. 1-18.
10. Warrington, C., (2006). *Finite element modeling for tap design improvement in form tapping*, Journal of Manufacturing Science and Engineering, vol 128, pp. 65-73.

---

Received: January 26, 2013 / Accepted: June 5, 2013 /  
Paper available online: June 10, 2013 © International  
Journal of Modern Manufacturing Technologies.